Liver Research 7 (2023) 124–135

Contents lists available at ScienceDirect

Liver Research

journal homepage: http://www.keaipublishing.com/en/journals/liver-research

Original Article

Glucokinase activator improves glucose tolerance and induces hepatic lipid accumulation in mice with diet-induced obesity☆

Nan Cai [a], Xuanrong Chen [a], Jia Liu [a], Zheyao Wen [a], Siyin Wen [a], Wen Zeng [a], Shuo Lin [a], Yanming Chen [a, b, c, d], Guojun Shi [a, b, c, d, *], Longyi Zeng [a, b, c, d, *]

[a] Department of Endocrinology and Metabolism, The Third Affiliated Hospital of Sun Yat-sen University, Guangzhou, Guangdong, China
[b] Guangdong Provincial Key Laboratory of Diabetology, Guangzhou, Guangdong, China
[c] Guangzhou Municipal Key Laboratory of Mechanistic and Translational Obesity Research, Guangzhou, Guangdong, China
[d] Medical Center for Comprehensive Weight Control, The Third Affiliated Hospital of Sun Yat-sen University, Guangzhou, Guangdong, China

ARTICLE INFO

Article history:
Received 31 January 2023
Received in revised form
18 April 2023
Accepted 30 May 2023

Keywords:
Non-alcoholic fatty liver disease (NAFLD)
Diabetes
Glucokinase activator (GKA)
High-fat diet (HFD)-induced obesity
Hepatic lipid accumulation
Unfolded protein response (UPR)

ABSTRACT

Background and aims: Type 2 diabetes mellitus remains a substantial medical problem with increasing global prevalence. Pharmacological research is becoming increasingly focused on personalized treatment strategies. Drug development based on glucokinase (GK) activation is an important strategy for lowering blood glucose. This study aimed to investigate the effect of GK activation on glucose and lipid metabolism in diet-induced obese mice.

Materials and methods: Mice were fed with a high-fat diet (HFD) for 16 weeks to induce obesity, followed by a GK activator (GKA, AZD1656) or vehicle treatment by gavage for 4 weeks. The effect of GKA treatment on glucose metabolism was evaluated using glucose and insulin tolerance tests. Hepatic lipid accumulation was assessed by hematoxylin and eosin staining, Oil Red O staining, and transmission electron microscopy. The underlying mechanism of GK activation in glucose and lipid metabolism in the liver was studied using transcriptomic analysis, with a mechanistic study in mouse livers *in vivo* and AML12 cells *in vitro*.

Results: GK activation by GKA treatment improved glucose tolerance in HFD-fed mice while increasing hepatic lipid accumulation. Transcriptomic analysis of liver tissues indicated the lipogenesis and protein kinase RNA-like endoplasmic reticulum kinase (PERK)-unfolded protein response (UPR) pathway activations in GKA-treated HFD-fed mice. Inhibition of the ACC activity, which is an important protein in lipogenesis, attenuated GKA treatment-induced lipid accumulation and PERK-UPR activation *in vitro*.

Conclusions: GK activation improved glucose tolerance and insulin sensitivity while inducing hepatic lipid accumulation by increasing the lipogenic gene expression, which subsequently activated the hepatic PERK-UPR signaling pathway.

1. Introduction

Approximately two-fifths of individuals globally are reported to be overweight or obese,[1] which is a major risk factor for metabolic disorders such as non-alcoholic fatty liver disease (NAFLD) and type 2 diabetes mellitus (T2DM). NAFLD has emerged as the leading chronic liver disease worldwide and is linked to non-alcoholic steatohepatitis (NASH), fibrosis, cirrhosis, and hepatocellular carcinoma,[2–4] as well as T2DM.[5,6] NAFLD has been reported to double the risk of developing T2DM, independent of obesity and other metabolic risk factors.[7] A recent study revealed that around 50% of the patients with NAFLD would suffer from T2DM within 20 years.[8] Moreover, the majority of patients suffering from NASH die due to T2DM and/or cardiometabolic disease complications.[9] About one-fifth of the global population suffered from NAFLD,[3,10] of which 56% were diagnosed with T2DM,[11] and the number of patients with both T2DM and NAFLD is estimated to continuously increase.

☆ Edited by Peiling Zhu.

* Corresponding authors. Department of Endocrinology and Metabolism, The Third Affiliated Hospital of Sun Yat-sen University, Guangzhou, Guangdong, China.
E-mail addresses: shigj6@mail.sysu.edu.cn (G. Shi), zengly@mail.sysu.edu.cn (L. Zeng).

https://doi.org/10.1016/j.livres.2023.05.003

Glucokinase (GK) is the first rate-limiting enzyme of glycolysis and is abundantly expressed in the hepatocytes that control hepatic glucose uptake and glycogen synthesis, while its activity is tightly regulated by the GK regulatory protein depending on the metabolic status.[12] Genetic mutations causing gain or loss of function in GK cause critical impacts, such as permanent neonatal diabetes mellitus (PNDM), maturity-onset diabetes of the young, or hyperinsulinemia.[13] GK activators (GKAs) are a class of chemicals that bind to an allosteric site on GK and increase its enzymatic activity. GKA treatment has been proposed as a potential therapeutic strategy for T2DM,[14,15] as it was reported to promote insulin release and improve insulin sensitivity.[13] However, challenges emerged from phase 2 trials during the clinical development of GKAs for T2DM, such as hypoglycemia-related side effects, unsustainable efficacy, and other adverse reactions. AZD1656, which is a GKA developed by AstraZeneca, was well-tolerated in patients with T2DM and is effective in lowering blood glucose.[13] AZD1656 also reduced the mortality rate in patients with DM who were infected with severe acute respiratory syndrome coronavirus 2.[16] The liver is responsible for lowering postprandial blood glucose after GKA treatment.[17,18] However, the effect of GKA treatment on hepatic lipid metabolism is unclear.

The endoplasmic reticulum (ER) plays a vital role in lipid and protein synthesis in mammalian cells, and ER homeostasis is crucial for physiological function. However, ER homeostasis can be disturbed by factors such as hyperlipidemia, hyperglycemia-induced excess reactive oxygen species generation, inflammation, viruses, drugs, etc.[19] The unfolded protein response (UPR) restores ER homeostasis by decreasing protein translation, increasing protein folding capacity, degrading misfolded proteins, etc.[20] The three major branches of the mammalian UPR pathways include protein kinase RNA-like ER kinase (PERK), inositol-requiring enzyme 1alpha (IRE1α), and activating transcription factor 6 (ATF6) signaling pathways.[21] Associations between ER stress and metabolic diseases, such as NAFLD and T2DM, were observed in the livers of patients with NAFLD and obesity,[22,23] and reports revealed that increased expression levels of ER stress-related genes were significantly reduced in patients after weight loss.[24,25] The PERK signaling pathway, as an important component of the UPR pathways, restores ER homeostasis mainly by inhibiting protein synthesis and is involved in NAFLD progression.[26,27] Chronic ER stress not only harms the function and survival of pancreatic beta (β) cells in T2DM pathogenesis but also causes hepatic insulin resistance.[28] A recent study demonstrated that GK activation could alleviate ER stress-induced pancreatic β cell death.[29] However, the relationship between hepatic GK activation and the ER stress response remains unclear.

This present study aimed to investigate the effect of GKA treatment on glucose and lipid metabolism in high-fat diet (HFD)-fed mice with obesity, as well as in regulating the hepatic ER stress response.

2. Materials and methods

2.1. Ethical approval

This study complied with the Declaration of Helsinki and was approved by the Institutional Animal Care and Use Committee of Sun Yat-sen University (No. SYSU-IACUC-2021-000623). All animal procedures were conducted following the Animal Care and Use Guidelines of Sun Yat-sen University.

2.2. Animals and treatments

Male C57BL/6J mice (6-week-old) were purchased from GemPharmatech Company (Nanjing, China). This study only used male mice as female mice are resistant to diet-induced obesity and metabolic syndrome.[30,31] Body weight and random blood glucose of mice were measured at 8 weeks of age. Then, mice were randomly divided into two groups (n = 10 for each group) and were fed a standard chow diet (CD) or HFD (60% fat, 20% carbohydrate, and 20% protein; Research Diets #D12492, New Brunswick, NJ, USA) respectively for 16 weeks. Each group of mice was then randomly divided into two groups (n = 5 for each group) based on their body weight, random glucose, and fasting glucose for treatment with GKA (AZD1656, #919783-22-5, Ariel Chemical Technology, Wuhan, China) or vehicle control, respectively. GKA was resolved in 0.1% CMC-Na and 0.1% Tween-80 (#9004-32-4 and #9005-65-6, respectively, MedChemExpress, Monmouth Junction, NJ, USA), and was orally given at 2 mg/kg daily.[32] After 4 weeks of treatments, mice were sacrificed for further analysis after overnight fasting. All mice were housed in a 12 h light and 12 h dark cycle, maintained at 25 °C, and free access to drinking water and food.

2.3. Intraperitoneal glucose tolerance test (IPGTT), oral glucose tolerance test (OGTT), and insulin tolerance test (ITT)

Food was withdrawn from each cage with clean beddings a day before IPGTT or OGTT. The mice were fasted for 16 h, followed by intraperitoneal injection or gavage with 20% (w/v) glucose in saline solution at 2 g/kg body weight, and blood glucose levels were measured via tail veins at the indicated time points. The mice were given AZD1656 at 2 mg/kg 30 min before the test for OGTT,[33] and blood glucose levels were measured via tail veins at the indicated time points (#84629341, Glucose Test Strips, Bayer, Leverkusen, Germany). The mice were given 1.5 U/kg of recombinant human insulin (Humulin, Eli Lilly and Company, Indianapolis, IN, USA) for ITT after 6 h fasting, and blood glucose levels were measured via tail veins at the indicated time points.

2.4. Histological analysis

Liver sections were embedded in paraffin and stained with hematoxylin and eosin (H&E) for morphological analysis. Oil Red O staining was applied to analyze lipid droplet accumulation in frozen liver sections. Images were acquired with a microscope (Olympus, Tokyo, Japan), and Image J software was used to measure the areas and diameters of lipid droplets.

2.5. Western blot

Total protein was isolated from tissues or cells in radioimmunoprecipitation assay (RIPA) lysis buffer and protein concentrations were determined with a BCA Protein Assay Kit (Thermo Fisher Scientific, Waltham, MA, USA). Each sample of 20 μg of protein was subjected to 10% SDS-PAGE gel analysis, transferred to a polyvinylidene difluoride membrane, and incubated with corresponding primary antibodies overnight at 4 °C. The bands were visualized with a ChemiDoc MP Imaging System (Bio-Rad, Hercules, CA, USA) after incubation with secondary antibodies (Jackson ImmunoResearch, Philadelphia, PA, USA). Protein expression levels were quantified with Image Lab software and normalized to the heat shock protein 90 (HSP90). AKT (#9272), phosphorylated (p)-AKT (#4060), HSP90 (#4874), acetyl-CoA carboxylase (ACC, #3662), PERK (#3192), p-eIF2α (#3597), eIF2α (#5324), ATF4 (#11815), and CCAAT/enhancer binding protein (C/EBP) homologous protein (CHOP, #5554) were purchased from Cell Signaling Technology (Danvers, MA, USA). Glycogen synthase kinase 3beta (GSK3β, #AF5026) and p-GSK3β (#AF2016) were purchased from Affinity Biosciences (Changzhou, China).

2.6. Transcriptomic analysis and quantitative real-time polymerase chain reaction (q-PCR)

Total RNA was extracted from liver tissues with an RNeasy Micro Kit (Qiagen, Hilden, Germany) and quantified by the NanoDrop 2000 (Thermo Fisher Scientific, Waltham, MA, USA). RNA integrity and genomic DNA contamination were tested by denaturing agarose gel electrophoresis. RNA sequencing (RNA-seq) was performed by the MustSeq 3′mRNA DEG Kit (Sequmed Biotech, Guangzhou, China) and sequenced on HiSeq 2500 sequencing system (Illumina, CA, USA). Data quality was demonstrated using FastQC V 0.22.8, and the reads of sorted bam files were counted using FeatureCounts. Fragments per kilobase of transcript per million mapped reads (FPKM) for MustSeq were calculated to normalize the results and build an expression matrix for statistical and functional analysis. For q-PCR, total RNA was isolated using TRIzol reagent (#T9424, Sigma-Aldrich, Saint Louis, MO, USA), and cDNA was synthesized with a PrimeScript RT Reagent Kit with gDNA Eraser (#RR047,TAKARA), q-PCR was performed using the SYBR Green Premix Pro Taq qPCR kit (#AG11718, Accurate Biology) following the manufacturer's instruction. The primer sequences used are listed as follows: Perk forward, 5′-TCAAGTTTCCTC-TACTGTTCACTCA-3′, reverse, 5′-CGGGAAACTCCAAGTTCTCA-3′; β-actin forward, 5′-GTCCACCCCGGGGAAGGTGA-3′, reverse, 5′-AGGCCTCAGACCTGGGCCATT-3′; Atf4 forward, 5′-GGGTTCTGTCT TCCACTCCA-3′, reverse, 5′-AAGCAGCAGAGTCAGGCTTTC-3′.

2.7. Generation of the heatmap, correlation heatmap, and graphical abstract

The heatmap was generated from the ImageGP platform (http://www.ehbio.com/ImageGP/index.php/Home/Index/index.html) after uploading the raw data following the manufacturers' instructions. The correlation heatmap was generated by the Genescloud platform (https://www.genescloud.cn/home). All elements of the graphical abstract were from Biorender (https://biorender.com/). The Pearson correlation coefficient of ER stress-related genes, UPR-related genes, and lipogenesis-related genes was analyzed based on the gene expression data (FPKM) using Pearson correlation analysis. *P*-values of <0.05 were considered significant.

2.8. Metabolic and liver function assays

Plasma triglyceride (TG), total cholesterol, alanine aminotransferase (ALT), and aspartate aminotransferase (AST), as well as liver TG, were measured using corresponding commercial kits (Nanjing Jiancheng Bioengineering Institute, Nanjing, China) with liver tissue or serum samples according to the manufacturer's instructions. Homeostatic model assessment for insulin resistance (HOMA-IR) and HOMA-β were calculated as described.[34] The mice were fasted overnight and were intraperitoneally injected with poloxamer P-407 (#IP9010, Beijing Solarbio Science & Technology Co., Ltd., Beijing, China) at 1 g/kg in saline to inhibit very low-density lipoprotein (VLDL) catabolism for VLDL-TG secretion assay. Fifty microliters of blood were collected from the retro-orbital plexus in heparinized tubes at the indicated time points and assayed for plasma TG (#A110-1-1, Nanjing Jiancheng Bioengineering Institute, Nanjing, China) following the manufacturer's instructions.

2.9. Cell culture

The mouse hepatocyte cell line AML12 was kindly donated by Dr. Wei Luo (Jinan University, Guangzhou, China). The cells were cultured in a standard medium comprising F12K, 10% fetal bovine serum, 1% penicillin–streptomycin, and 1% insulin-transferrin-selenium (ITS, #I3146, Sigma-Aldrich, Saint Louis, MO, USA) and were maintained in a humidified 5% CO_2 atmosphere at 37 °C. Palmitic acid (PA) powder (#P9767-5g, Sigma-Aldrich, Saint Louis, MO, USA) or control (BSA, #A1933-5g, Sigma-Aldrich, Saint Louis, MO, USA) was dissolved in 0.01 mol/L of NaOH to make a stock solution. AML12 cells were treated with BSA/PA, with or without AZD1656 (5 μmol/L) and ACC inhibitor (ACCi, #PF-05175157, Selleck Chemicals, Houston, TX, USA). A commercially available colorimetric assay kit (Nanjing Jiancheng Bioengineering Institute, Nanjing, China) has been utilized to measure intracellular TG levels.

2.10. Total TG quantification

Briefly, TG was extracted from AML12 cells. The cells were vortexed with 500 μL of chloroform/methanol (3:2; v:v) solution after suspending in 100 μL of lysis buffer. The lower phase was dissolved in isopropanol after centrifugation for approximately 10 min. TG was performed according to the manufacturer's instructions (TG colorimetric assay kit, #A110-1-1, Nanjing Jiancheng Bioengineering Institute, Nanjing, China).

2.11. Statistical analysis

Statistical analysis was performed using GraphPad Prism 6.0 software (San Diego, CA, USA). Statistical parameters, including the value of *n*, are noted in figure legends. All data are presented as mean ± standard deviation (SD) unless specially stated. Statistical analysis between the two groups was analyzed by unpaired students' *t*-test. The correlation heatmap used the Pearson correlation analysis, and *P*-values of <0.05 were considered statistically significant.

3. Results

3.1. GK activation improves glucose tolerance in HFD-fed mice

A mouse model with HFD-induced obesity was established to study the effect of GKA treatment on glucose and lipid metabolism in obese mice. Based on the animal experimental design (Fig. 1A), body weight was measured twice a week. The body weight of obese mice was significantly higher than those of CD mice after 16 weeks of feeding (Fig. 1B). Impaired glucose tolerance (Fig. 1C) and insulin sensitivity (Fig. 1D and Supplementary Table 1) were observed in HFD-fed mice, which confirmed the successful diet-induced obese model establishment. CD and HFD-fed mice were divided into four groups (CD + vehicle, CD + GKA, HFD + vehicle, and HFD + GKA) after 16 weeks of feeding. GKA (AZD1656) or vehicle was orally administered for 4 weeks. Glucose tolerance was significantly improved after 4 weeks of GKA treatment following previous reports (Fig. 1E and F).[33] Moreover, improved ITT results were also observed (Fig. 1G–I). Interestingly, after normalization to initial glucose level, GKA treatment showed different trends of insulin sensitivity at 30 min and 90 min post insulin injection (Fig. 1I), suggesting that GKA might not significantly improve insulin resistance under HFD, beyond its glucose-lowering effect. Next, fasting insulin and glucose levels were measured (Fig. 1J and K). Expectedly, fasting glucose levels were significantly reduced by GKA treatment in HFD-fed mice. Although significant improvement in the HOMA-β index (Fig. 1L) was observed in the GKA-treated group under either CD or HFD feeding conditions, no difference was observed in fasting insulin levels and insulin resistance index (HOMA-IR, Fig. 1M) in GKA-treated mice, indicating that GK activation improved islet β cell function in HFD-fed mice.

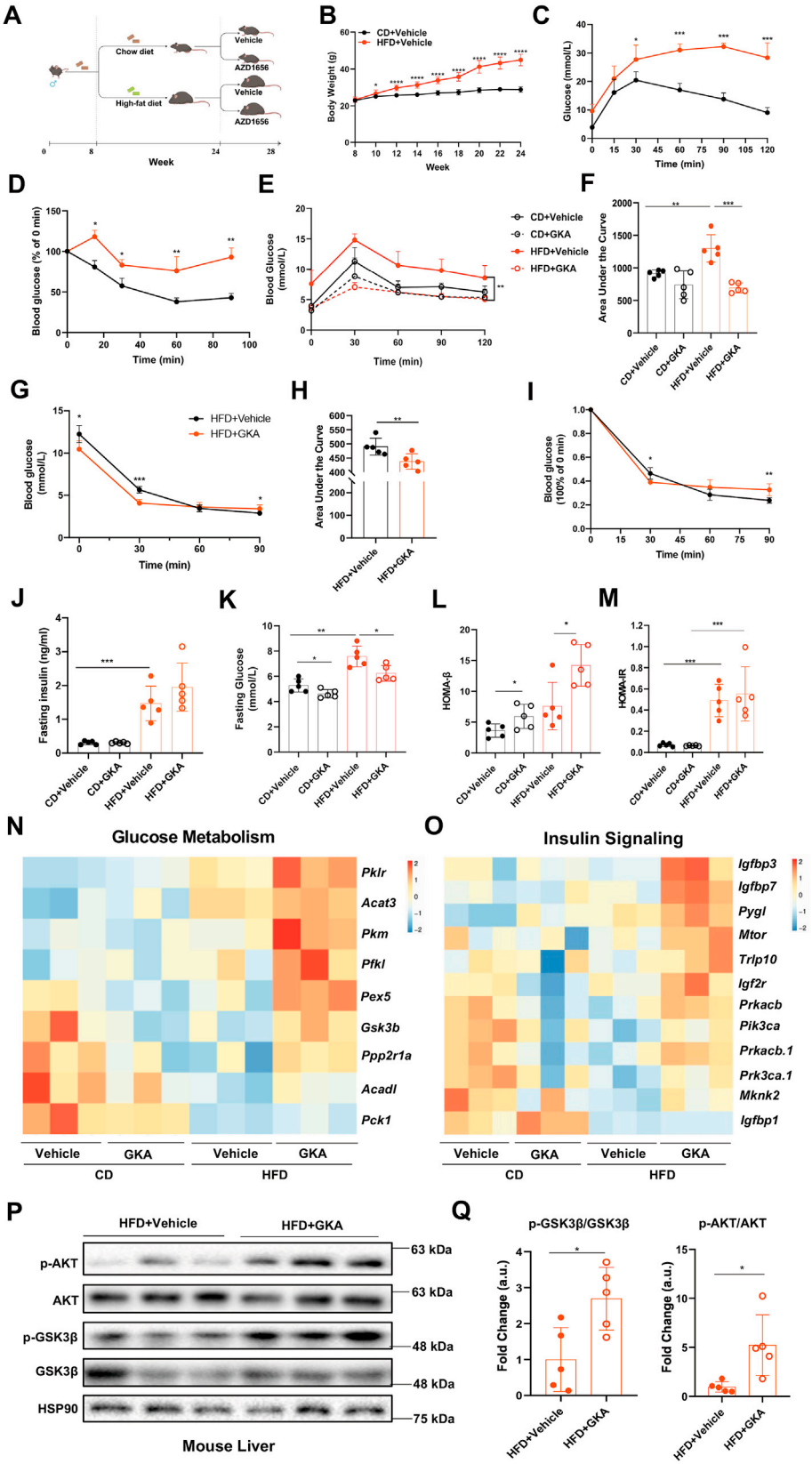

Fig. 1. GKA treatment improved glucose tolerance in diet-induced obese mice. **(A)** Cartoon of the experimental design. **(B)** The body weight of the chow diet (CD) and high-fat diet (HFD) fed mice (n = 10 for each group). **(C, D)** IPGTT and ITT of mice fed an HFD or CD for 16 weeks (n = 4–5 for each group). **(E, F)** OGTT analysis of mice with different treatments for 4 weeks, indicated as CD + Vehicle, CD + GKA, HFD + Vehicle, and HFD + GKA. AUC was shown in (F) (n = 5 for each group). **(G)** ITT and **(H)** AUC as well as **(I)** normalized ITT analysis after 30 days of glucokinase activator (GKA, AZD1656) treatment (n = 5 for each group). **(J)** The fasting plasma insulin and **(K)** fasting blood glucose levels were analyzed as indicated (n = 5 for each group). **(L)** HOMA-β and **(M)** HOMA-IR were calculated accordingly as described in the "materials and methods" section (n = 5 for each group). The heatmaps of **(N)** glucose metabolism and **(O)** insulin signaling pathway related genes from indicated groups of mice were demonstrated from transcriptomic analysis

We proposed the important role of the liver in the improved glucose tolerance observed following GKA treatment because GKA treatment reduced fasting blood glucose without affecting insulin secretion. RNA-Seq analysis was performed with liver samples to understand the mechanistic role of GKA in regulating glucose metabolism in the liver. The results revealed that GKA treatment significantly changed hepatic genes-related to glucose metabolism and insulin signaling (Fig. 1N and O). The protein levels-related to glycogen synthesis and insulin signaling were analyzed in mouse liver tissues (Fig. 1P and Q), confirming that insulin signaling and glycogen synthesis were activated by GKA treatment under HFD feeding. These results showed that GKA treatment improved glucose tolerance possibly through increasing hepatic insulin signaling and glycogen synthesis.

3.2. GK activation aggravated hepatic lipid accumulation in mice with diet-induced obesity

Plasma TG and liver weight were analyzed to understand the effect of GKA treatment on general liver physiology. GKA treatment significantly reduced plasma TG in mice under HFD (Fig. 2A); however, the liver weight and liver/body weight ratio were significantly increased (Fig. 2B and C), indicating more lipid accumulation after GKA treatment under HFD feeding. Thus, hepatic TG levels were measured, and the data confirmed the increased hepatic TG after GKA treatment in HFD-fed mice (Fig. 2D). Further, pathological changes in liver sections were examined (Fig. 2E–H). Both H&E staining and Oil Red O staining confirmed the increased lipid area (Fig. 2E and F), and transmission electron microscopy (TEM) technique observed larger lipid droplet diameters (Fig. 2E and H) after GKA treatment in HFD-fed mice. Increased ALT and AST levels also indicated an exacerbation of lipid accumulation induced hepatocyte injury after GKA treatment in HFD-fed mice (Fig. 3A).

Beyond the increased lipid area, the increased ballooning area was also observed in GKA-treated mice fed with HFD compared with vehicle control (Fig. 3B), accompanied by increased mRNA expression levels related to liver inflammation and fibrosis (Fig. 3C and D). NAFLD activity score (NAS), including ballooning, inflammation, and steatosis, was used to evaluate morphological changes in the liver to understand the pathological changes induced by GKA treatment in addition to lipid analysis (Fig. 3E). The ballooning and steatosis scores in the GKA-treated group were significantly higher than those in the obese vehicle control group. Interestingly, increased lipid accumulation after GKA treatment was not observed in mice fed on CD. These data indicated that GKA treatment induced hepatic lipid accumulation and hepatocyte injury in mice with HFD-induced obesity.

3.3. GK activation increased lipogenesis in diet-induced obese mice

Hepatic TG metabolism includes fatty acid uptake, *de novo* lipogenesis, fatty acid oxidation, and lipid transport. Lipid accumulation in the liver could be attributed to increased fatty acid uptake and *de novo* lipogenesis, or decreased fatty acid oxidation and VLDL secretion. We performed a transcriptomic analysis of liver samples to investigate the mechanistic role of GKA treatment in lipid accumulation under HFD conditions. The differentially expressed genes were analyzed by Gene Ontology (GO) enrichment, which confirmed the involvement of altered lipid metabolism profiles after GKA treatment under HFD conditions (Fig. 4A). “Regulation of the lipid biosynthetic process”, “fatty acid metabolic process”, “carboxylic acid biosynthetic process”, etc., were ranked among the top enriched pathways. Thus, differentially expressed genes related to lipogenesis with GKA treatment from both CD and HFD conditions, including sterol regulatory element-binding transcription factor 1 (*Srebf1*), fatty acid synthase (*Fasn*), stearoyl-CoA desaturase 1 (*Scd1*), and acetyl-CoA carboxylase alpha (*Acaca*),[35] are illustrated in a heatmap (Fig. 4B). Furthermore, the heatmap displays the genes related to fatty acid metabolism, including genes involved in regulating mitochondrial function (Fig. 4C). Key genes involved in fatty acid uptake, VLDL secretion, and VLDL assembling were also demonstrated (Fig. 4D–F).[36] Interestingly, with GKA treatment, no significant changes were observed in VLDL assembly-related genes and fatty acid uptake-related genes exept for solute carrier family 27 member 5 (*Slc27a5*) (Fig. 4D),[37] while VLDL secretion-related genes were significantly upregulated (Fig. 4E). The capability of VLDL-TG secretion was confirmed by the VLDL-TG secretion assay (Fig. 4G). A rising trend in TG content was found at 180 min, indicating that VLDL-TG secretion was not significantly inhibited and was not the main underlying contributor. Hence, increased *de novo* lipogenesis was the main source of hepatic TG content. To further clarify the relationship between these factors, we analyzed the correlation between hepatic *Acaca* mRNA levels and hepatic TG levels (Fig. 4H), which confirmed that increased *de novo* lipogenesis was the main source of hepatic TG. Additionally, the increases in the NAS and hepatic enzymes ALT and AST were related to the increase in hepatic *Acaca* mRNA levels (Fig. 4I–K), which demonstrated that TG accumulation impaired hepatic function. The increase of ACC protein expression in the livers of obese mice and in AML12 cells demonstrated that GK increased *de novo* lipogenesis (Fig. 4L and M). These results demonstrated that lipid accumulation by GKA treatment could be mediated via lipogenesis.

3.4. GK activation induced lipogenesis and triggered the PERK-UPR pathway in obese mice and PA-treated AML12 cells

Lipid accumulation induced a series of changes in hepatocytes, such as hepatic steatosis, inflammation, and ER stress. The ER is important for hepatic lipid metabolism regulation as the major organelle for lipid synthesis, while perturbed ER homeostasis (ER stress) mediates hepatic steatosis.[19] The GO enrichment analysis of the hepatic transcriptomic data under GKA treatment with HFD feeding indicated ER proteins among the top cellular components in mediating the GKA effect (Fig. 5A). Relative mRNA expression levels of ER-associated genes were shown in detail in a heatmap (Fig. 5B). Besides, correlation heatmap analysis demonstrated that increased mRNA levels of lipogenic genes were significantly correlated with the expression levels of ER-related genes (Fig. 5C). Considering the critical role of ER stress and UPR signaling pathway in hepatic lipid accumulation, UPR signaling pathways may be involved in GKA-induced lipid accumulation under HFD feeding. Indeed, the correlation heatmap indicated a significant association between lipogenic genes and UPR signaling, particularly the PERK pathway-associated genes (Fig. 5D). Further, a significant correlation was observed between hepatic TG levels or

($n = 3$ for each group). **(P, Q)** Protein expressions of the insulin signaling pathway were determined by Western blot, with quantification shown in (Q) ($n = 3$ for each group). Data are presented as the mean ± standard deviation (SD), $^{*}P < 0.05$, $^{**}P < 0.01$, $^{***}P < 0.001$, $^{****}P < 0.0001$. Abbreviations: Acadl, acyl-CoA dehydrogenase long chain; AUC, area under the curve; GSK3β, glycogen synthase kinase 3beta; HOMA-IR, homeostatic model assessment for insulin resistance; HSP90, heat shock protein 90; Igfbp, insulin-like growth factor binding protein; Igf2r, insulin-like growth factor 2 receptor; IPGTT, intraperitoneal glucose tolerance test; ITT, insulin tolerance test; Mknk2, MAP kinase interacting serine/threonine kinase 2; Mtor, mechanistic target of rapamycin; OGTT, oral glucose tolerance test; Pck1, phosphoenolpyruvate carboxykinase 1; Pfkl, liver-type subunit of phosphofructokinase; Pklr, pyruvate kinase; Pkm, pyruvate kinase M; Prkacb, protein kinase cAMP-activated catalytic subunit beta; Pygl, glycogen phosphorylase L.

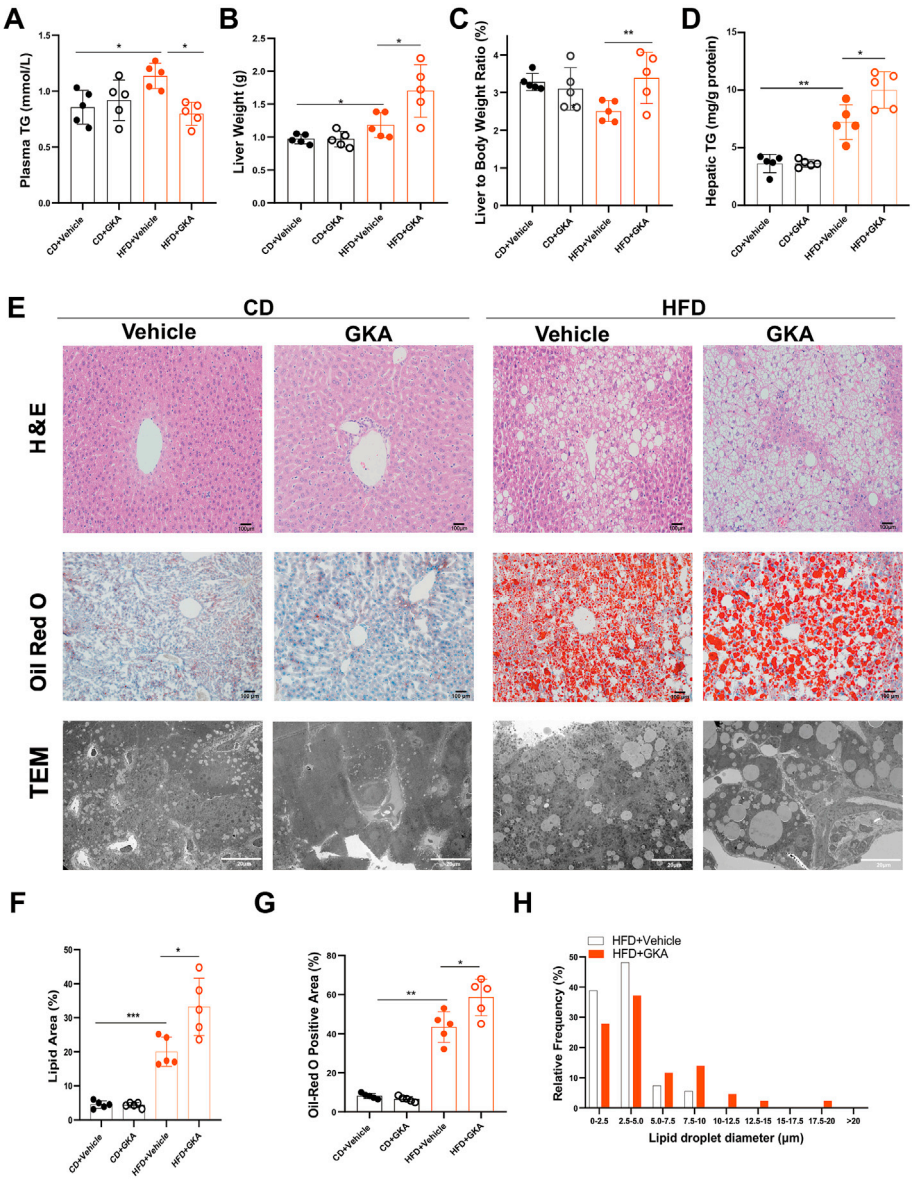

Fig. 2. GKA treatment aggravated hepatic lipid accumulation in diet-induced obese mice. **(A)** Plasma TG, **(B)** liver weight and **(C)** liver/body weight ratio, and **(D)** hepatic TG content were measured from mice of each group as indicated. **(E)** H&E staining (scale bar = 100 μm), Oil Red O staining (scale bar = 100 μm), and TEM (scale bar = 20 μm) of liver samples from mice of each group as indicated. The lipid area of liver tissues was examined by **(F)** H&E and **(G)** Oil Red O staining. **(H)** TEM technique was applied to understanding the size of lipid droplet. Data are presented as the mean ± standard deviation (SD), $^{*}P < 0.05$, $^{**}P < 0.01$, $^{***}P < 0.001$. $n = 3–5$ for each group. Abbreviations: CD, chow diet; GKA, glucokinase activator; H&E, hematoxylin and eosin; HFD, high-fat diet; TEM, transmission electron microscopy; TG, triglyceride.

NAS and the mRNA expression levels of the PERK pathway-associated genes, *Eif2ak3* (*Perk*) and *Atf4* (Fig. 5E–G). The PERK signaling pathway activation was also confirmed in the liver by Western blot analysis in GKA-treated obese mice, as well as GKA-treated AML12 hepatocytes under PA treatment (Fig. 5H and I). These results indicated the PERK signaling pathway activation by GK activation under HFD feeding *in vivo* or hyperlipidemia conditions *in vitro*.

3.5. Inhibition of lipogenesis reduced intracellular TG content and alleviated PERK-UPR pathway in PA-treated AML12 cells in vitro

Excessive cellular lipid accumulation could induce ER stress, and GKA treatment neither activated ER stress signaling in the basal conditions in AML12 cells, or CD-fed mice. GKA treatment increased the mRNA and protein levels of *Acaca* (ACC) in HFD-fed mice, which initiates lipogenesis, thus it was hypothesized that *Acaca* upregulation might be involved in GKA treatment-induced lipid accumulation. GKA pretreatment increased intracellular TG levels under PA incubation in AML12 cells (Fig. 6A), and ACCi co-pretreatment reversed GKA-induced TG accumulation under PA or vehicle incubation. GKA treatment increased the protein level of ACC as well as the downstream target of PERK-UPR signaling, ATF4 (Fig. 6B–D). ACC inhibition alleviated the PERK-UPR pathway activation induced by GKA under PA treatment or basal conditions (Fig. 6D). Overall, our data suggest that GKA treatment induced hepatic lipid accumulation under hyperlipidemia conditions, and excessive lipid in hepatocytes might be responsible for triggering the PERK signaling pathway, which is illustrated by our hypothetic model (Fig. 6E).

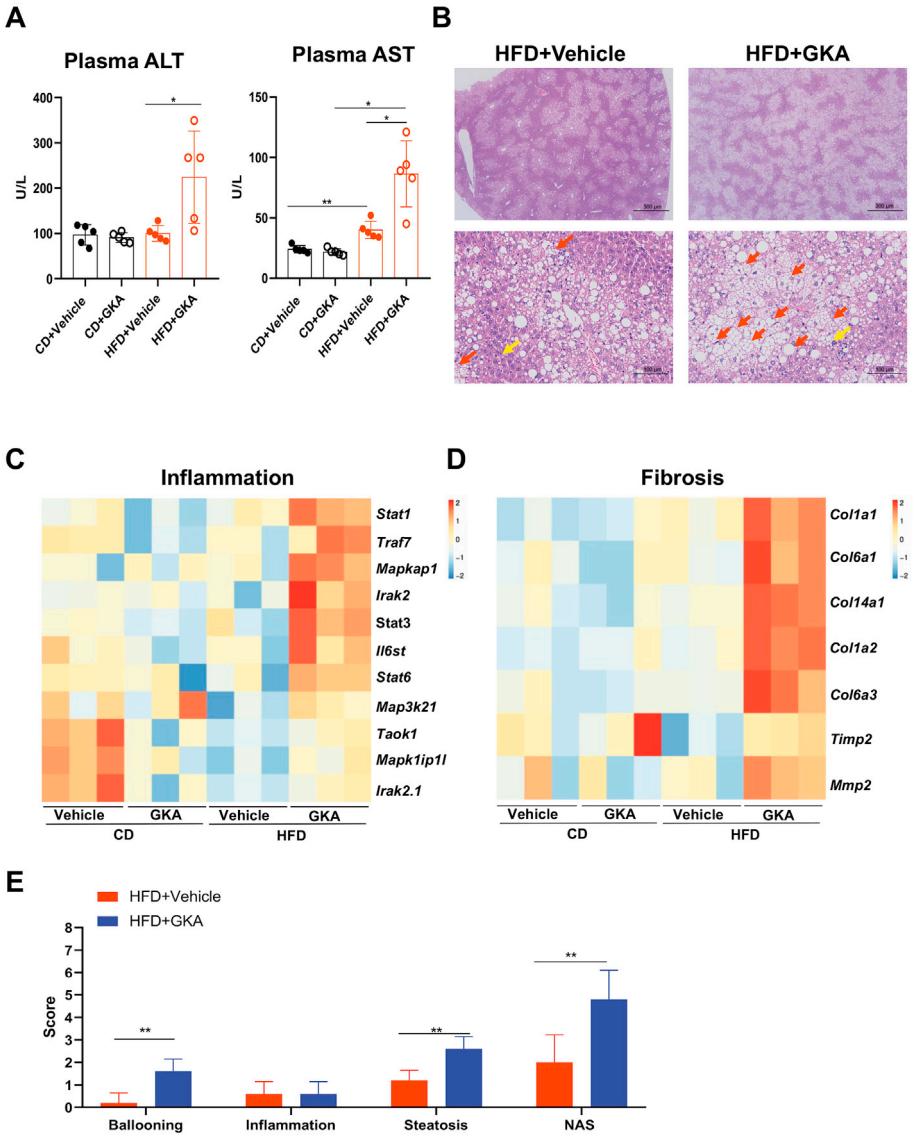

Fig. 3. GKA treatment induced hepatic pathological changes in mice with diet-induced obesity. (A) Plasma ALT and AST activities were analyzed from mice in each group as indicated. **(B)** The representative pathological changes in livers from mice of each group as indicated. Ballooning and steatosis were indicated by red and yellow arrows in H&E staining, respectively. The heatmaps of **(C)** liver inflammation and **(D)** fibrosis related genes from transcriptomic analysis of the indicated groups of mice ($n = 3$ for each group). **(E)** Quantitative analysis of liver pathology from mice of the indicated groups, including ballooning, inflammation, steatosis, and NAS. Data are presented as the mean ± standard deviation (SD), $^{*}P < 0.05$, $^{**}P < 0.01$. $n = 5$ for each group unless specifically mentioned. Abbreviations: ALT, alanine aminotransferase; AST, aspartate aminotransferase; CD, chow diet; Col, collagen; GKA, glucokinase activator; H&E, hematoxylin and eosin; HFD, high-fat diet; Il6st, interleukin 6 cytokine family signal transducer; Irak2, interleukin-1 receptor-associated kinase 2; Mapkap1, mitogen-activated protein kinase associated protein 1; Mapk1ip1l, mitogen-activated protein kinase 1 interacting protein 1 like; Mmp2, matrix metalloproteinase 2; NAS, non-alcoholic fatty liver disease (NAFLD) activity score; Stat, signal transducer and activator of transcription; Taok1, thousand and one amino acid kinase 1; Timp2, tissue inhibitor of metalloproteinase 2; Traf7, tumor necrosis factor receptor-associated factor 7.

4. Discussion

Our findings demonstrated that GK activation improved glucose tolerance in mice with diet-induced obesity while inducing hepatic lipid accumulation that triggers the PERK-UPR pathway. Improvements in both islet β cell function and insulin signaling were observed with GKA treatment, which might contribute to the improved glucose tolerance. We proposed that hepatic *de novo* lipogenesis might contribute to GKA treatment-induced lipid accumulation as lipid accumulation was observed only in HFD-fed mice in response to the GKA treatment but not in CD, whereas hepatic lipid uptake and export pathways were not among the top enriched pathways from transcriptomic analysis of GKA-treated mice. Liver tissue and AML12 cell analysis confirmed that the lipogenic pathway was activated under GKA treatment in HFD-fed mice. Additionally, the transcriptomic analysis suggested that UPR signaling pathways, particularly the PERK-eIF2α-ATF4 signaling, were activated due to excessive lipid accumulation. Finally, we noted that the lipogenesis inhibitor (ACCi) reduced TG levels in PA- and GKA-treated AML12 cells and alleviated the PERK-UPR signaling pathway.

The UPR signaling pathway was reported to be triggered by drugs, inflammation, viruses, etc.[19] Our study suggested that lipid accumulation through the ACC pathway under GKA treatment stimulated UPR signaling, consistent with a previous study that revealed excess lipids in the liver-activated UPR signaling.[38] Additionally, the significant correlation between the mRNA expression of lipogenesis-associated genes and the PERK signaling pathway in

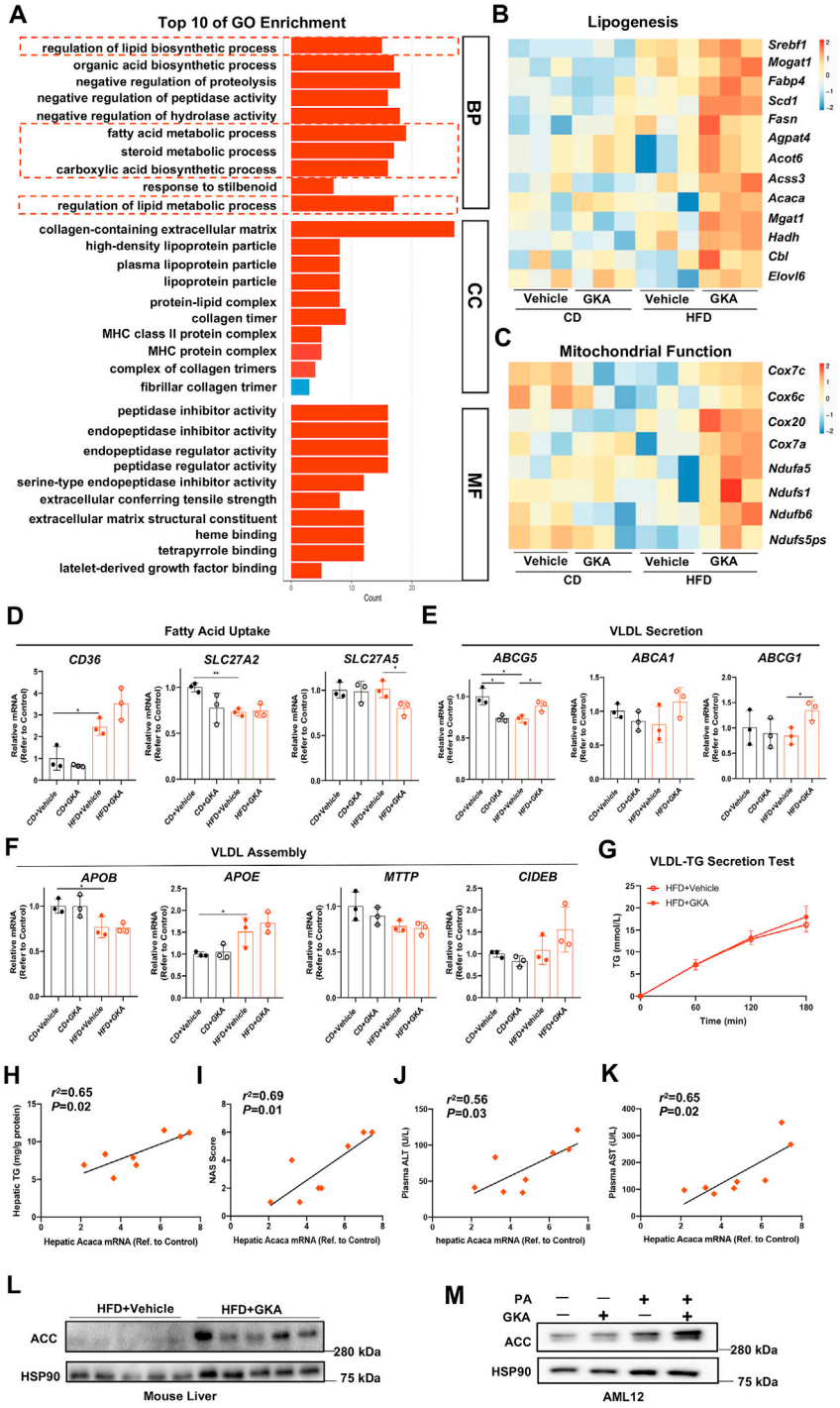

Fig. 4. GKA treatment increased hepatic lipogenesis in diet-induced obese mice and PA-treated AML12 cells. (A) Gene Ontology (GO) analysis of transcriptomic data from the livers of mice as indicated ($n = 3$ for each group). The heatmaps of **(B)** *de novo* lipogenesis and **(C)** mitochondrion function related genes from transcriptomic analysis of the indicated groups of mice ($n = 3$ for each group). The relative hepatic mRNA expressions of genes related to **(D)** fatty acid uptake, **(E)** VLDL secretion, and **(F)** VLDL assembling based on the FPKM value of transcriptomic analysis as indicated by each group ($n = 3$ for each group). **(G)** *In vivo* VLDL-TG secretion test was performed in HFD-Vehicle and HFD-GKA groups ($n = 3$ for each group). **(H–K)** The correlation analysis between relative hepatic Acaca mRNA expression levels and (H) hepatic TG content, (I) NAS, (J) plasma ALT activity, and (K) plasma AST activity ($n = 4$ for each group). **(L)** The protein level of ACC in mice with diet-induced obesity with GKA or vehicle treatment ($n = 5$ for each group). **(M)** The protein level of lipogenesis-related protein ACC in AML12 cells under treatments as indicated. Data are representative of three repeats. Data are presented as the mean ± standard deviation (SD), $^{*}P < 0.05$, $^{**}P < 0.01$. Abbreviations: ABC, ATP-binding cassette transporter; Acaca, acetyl-CoA carboxylase alpha; ACC, acetyl-CoA carboxylase; Acss3, acyl-CoA synthetase short chain family member 3; Agpat4, acylglycerophosphate acyltransferase 4; ALT, alanine aminotransferase; APO, apolipoprotein; AST, aspartate aminotransferase; BP, biological progress; CC, cellular component; CD, chow diet; CD36, cluster of differentiation 36; CIDEB, cell death-inducing DNA fragmentation factor 45 (DFF45)-like effector B; Elovl6, elongation of long chain fatty acid family member 6; Fabp4, fatty acid binding protein 4; Fasn, fatty acid synthase; FPKM, fragments per kilobase of transcript per million mapped reads; GKA, glucokinase activator; Hadh, 3-hydroxy acyl-CoA dehydrogenase; HFD, high-fat diet; HSP90, heat shock protein 90; MF, molecular function; Mgat1, monoacylglycerol O-acyltransferase 1; MHC, major histocompatibility complex; Mogat1, monoacylglycerol acyltransferase 1; MTTP, microsomal triglyceride transfer protein; NAS, non-alcoholic fatty liver disease (NAFLD) activity score; Ndufs1, NADH-ubiquinone oxidoreductase core subunit s1; PA, palmitic acid; Scd1, stearoyl-CoA desaturase 1; SLC27A, solute carrier 27A; Srebf1, sterol regulatory element-binding transcription factor 1; TG, triglyceride; VLDL, very low-density lipoprotein.

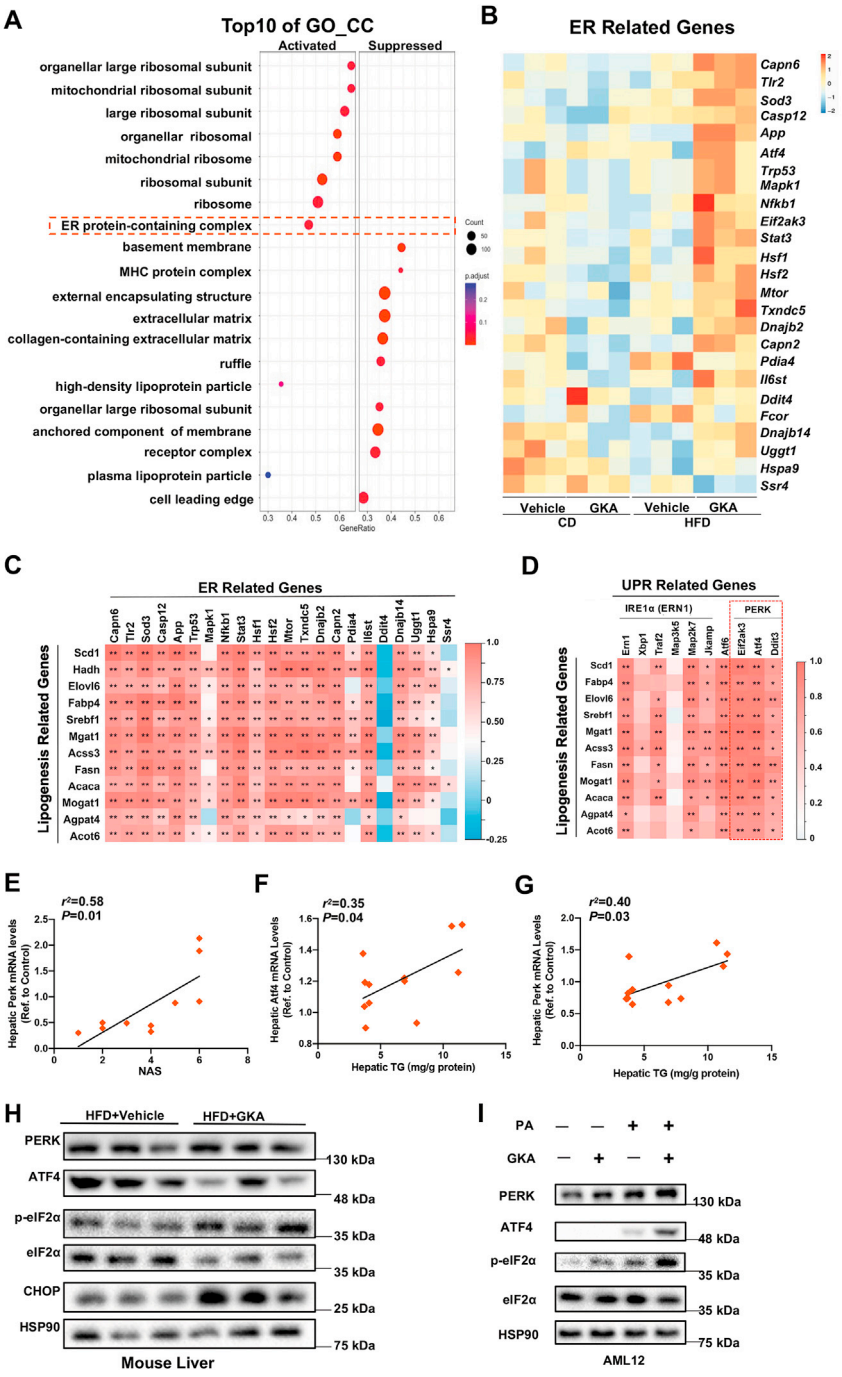

Fig. 5. Hepatic PERK-UPR pathway was activated in GKA-treated mice with diet-induced obesity and PA-treated AML12 cells. **(A)** GO analysis of top 10 activated and top 10 suppressed cellular components from liver transcriptomic analysis of GKA-treated mice with diet-induced obesity compared with the vehicle control. **(B)** The heatmap displayed the ER-related genes ($n = 3$ for each group). **(C, D)** The correlation heatmap between *de novo* lipogenesis-related genes and (C) ER-related genes or (D) UPR-related genes. **(E)** The correlation analysis between hepatic Perk mRNA expression (FPKM, from RNA-Seq analysis) and NAS in HFD-fed mice under GKA or vehicle treatment. **(F)** The correlation analysis between hepatic Atf4 mRNA expression (q-PCR) and hepatic TG content in obese mice. **(G)** The correlation analysis between hepatic Perk mRNA expression (q-PCR) and hepatic TG content in obese mice under GKA or vehicle treatment. **(H)** The hepatic protein levels of the PERK-UPR pathway in obese mice as indicated ($n = 3$ for each group). **(I)** The protein levels of PERK-UPR pathway in AML12 cells under treatment by PA and/or GKA; Data are representative of three repeats. $^{*}P < 0.05$, $^{**}P < 0.01$. Abbreviations: Acaca, acetyl-CoA carboxylase alpha; Acss3, acyl-CoA synthetase short chain family member 3; Agpat4, acylglycerophosphate acyltransferase 4; App, amyloid precursor protein; ATF, activating transcription factor; Capn, calpain; Casp12, caspase 12; CC, cellular component; CD, chow diet; CHOP, CCAAT/enhancer binding protein (C/EBP) homologous protein; Ddit, DNA damage-induced transcript; Eif2ak3, eukaryotic translation initiation factor 2 alpha kinase 3; Elovl6, elongation of long chain fatty acid family member 6; ER, endoplasmic reticulum; Fabp4, fatty acid binding protein 4; Fasn, fatty acid synthase; FPKM, fragments per kilobase of transcript per million mapped reads; GKA, glucokinase activator; GO, Gene Ontology; Hadh, 3-hydroxy acyl-CoA dehydrogenase; HFD, high-fat diet; HSF, heat shock factor; HSP90, heat shock protein 90; Il6st, interleukin 6 cytokine family signal transducer; IRE1α, inositol-requiring enzyme 1alpha; Mapk1, mitogen-activated protein kinase 1; Mgat1, monoacylglycerol O-acyltransferase 1; MHC, major histocompatibility complex; Mogat1, monoacylglycerol acyltransferase 1; Mtor, mechanistic target of rapamycin; NAS, non-alcoholic fatty liver disease (NAFLD) activity score; Nfkb1, nuclear factor kappa B subunit 1; PA, palmitic acid; Pdia4, protein disulfide isomerase family A member 4; PERK, protein kinase RNA-like ER kinase; q-PCR, quantitative real-time polymerase chain reaction; Scd1, stearoyl-CoA desaturase 1; Sod3, superoxide dismutase 3; Srebf1, sterol regulatory element-binding transcription factor 1; Ssr4, signal sequence receptor 4; Stat3, signal transducer and activator of transcription 3; TG, triglyceride; Tlr2, Toll-like receptor 2; Traf2, tumor necrosis factor receptor-associated factor 2; Txndc5, thioredoxin domain containing 5; Uggt1, UDP-glucose:glycoprotein glucosyltransferase; UPR, unfolded protein response; Xbp1, X-box binding protein 1.

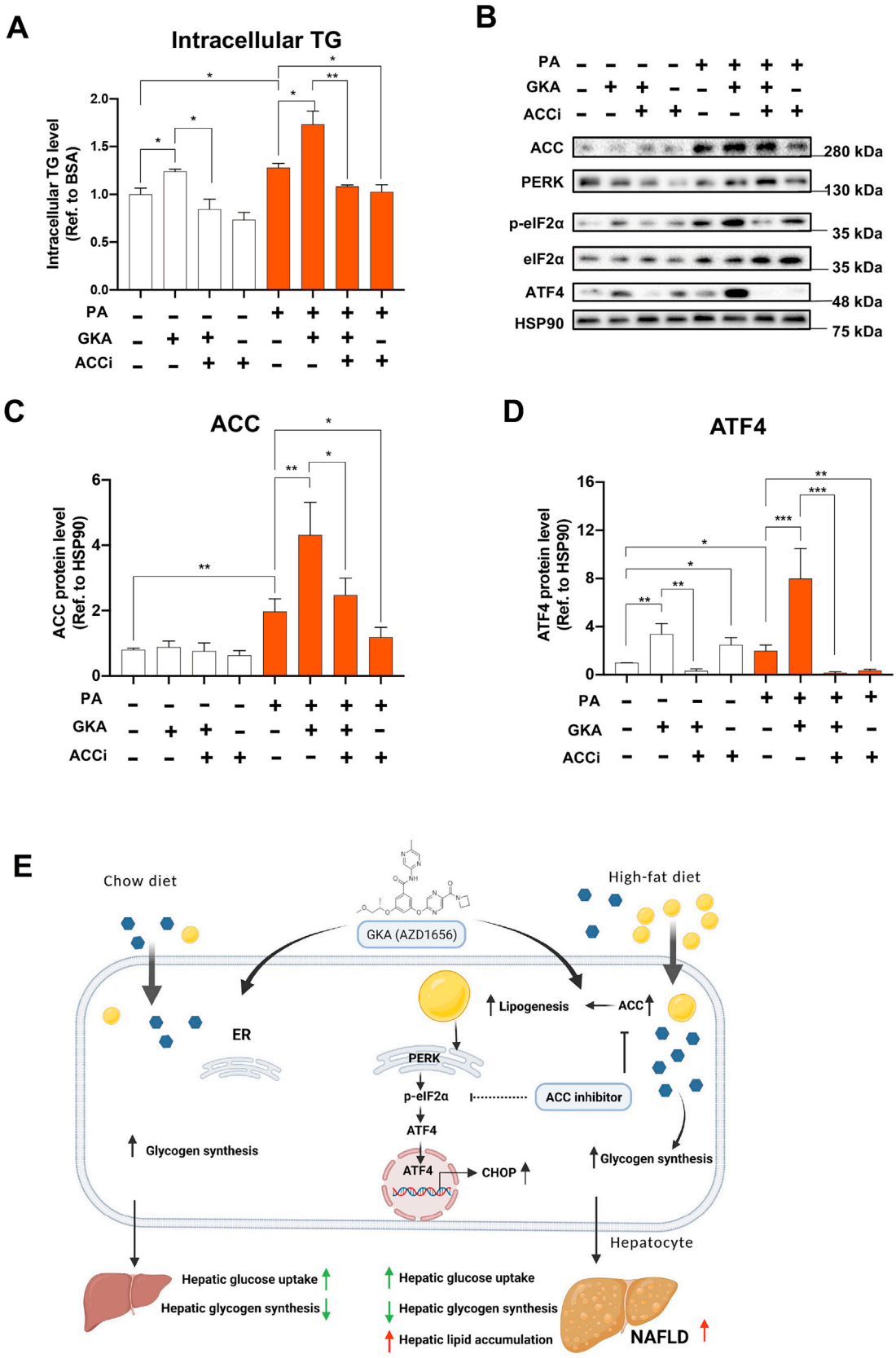

Fig. 6. Inhibition of lipogenesis-alleviated GKA treatment-induced lipid accumulation and inhibited the PERK-UPR pathway in AML12 cells. **(A)** Intracellular TG content and **(B)** protein expression levels of ACC and PERK-UPR pathway in AML12 cells under the treatment with PA, GKA, and ACCi as indicated. Quantification of **(C)** ACC and **(D)** ATF4 protein levels are shown. Data are representative of three repeats. Data are presented as the mean ± standard deviation (SD), $^{*}P < 0.05$, $^{**}P < 0.01$, $^{***}P < 0.001$. **(E)** Model illustrating the potential role of GKA in glucose and lipid metabolism. Abbreviations: ACCi, acetyl-CoA carboxylase inhibitor; ATF4, activating transcription factor 4; CHOP, CCAAT/enhancer binding protein (C/EBP) homologous protein; ER, endoplasmic reticulum; GKA, glucokinase activator; HSP90, heat shock protein 90; NAFLD, non-alcoholic fatty liver disease; PA, palmitic acid; PERK, protein kinase RNA-like ER kinase; TG, triglyceride; UPR, unfolded protein response.

GKA-treated HFD-fed mice, together with tissue protein analysis, indicated the activation of PERK-UPR signaling. Furthermore, the ACCi alleviated lipid accumulation and PERK signaling, suggesting that GKA-induced lipid accumulation was responsible for PERK signaling activation. However, the detailed signaling mechanism underlying GKA treatment-induced ACC expression requires further study, and a detailed signaling mechanism linking GKA treatment and PERK-UPR pathway activation remains to be uncovered. Reports showed that the PERK pathway played differential roles during NAFLD progression. Hepatic deletion of ATF4, which is downstream of the PERK pathway, attenuated NAFLD progression by attenuating *de novo* lipogenesis,[27] or by reducing cell death.[39] Another report demonstrated that C/EBP homologous protein induction through PERK signaling in macrophages prevented NAFLD progression.[40] Thus, the involvement of PERK pathway activation in mediating GKA treatment-induced hepatic lipid accumulation is an issue for further study.

Clinical trials have demonstrated that GKAs were effective in lowering blood glucose levels in patients with T2DM,[41–43] including the most recent clinical studies on a newly developed GKA, dorzagliatin.[13–15] The number of adverse events was similar between the treatment and placebo groups. However, a clear trend of increased plasma TG, as well as ALT/AST activity after 24 weeks of GKA treatment,[13] suggests its potential risk on liver function, and liver function status should be considered for GKA prescription. Our study revealed hepatic lipid accumulation with GKA treatment in HFD-fed but not CD-fed mice. Another study showed that GKA treatment only induced TG accumulation in db/db mice but not in lean mice.[44] Additionally, genetic studies have demonstrated that endogenous GK activation significantly increased the risk of NAFLD.[6,45,46] More studies on the role of GK activation in human subjects are required to pave the way for the clinical use of GKAs as GKA has been demonstrated as a potentially effective treatment for T2DM, and NAFLD progression is attributed to many factors, including genetic background, nutrition status, lifestyle, etc.[47]

5. Conclusions

In summary, the present study demonstrated that GK activation was effective in lowering blood glucose in mice with HFD-induced obesity, while it potentially raised the risk of increasing hepatic lipid accumulation that triggered the PERK-UPR pathway. Thus, liver function should be considered for patients if GKAs are considered for prescription. Combined with the recent progress on the effectiveness of GKAs in treating patients with T2DM and coronavirus disease 2019, more clinical studies or observations may be needed before GKAs may be used most advantageously in treating patients for personalized therapy.

Authors' contributions

N. Cai and X. Chen contributed equally to this work. N. Cai and X. Chen performed most of experiments and drafted the manuscript. J. Liu, Z. Wen, and S. Wen provided materials and assistance in the experiments. W. Zeng and S. Lin provided critical suggestions in experimental design and operations. Y. Chen provided funding support and critical suggestions. G. Shi and L. Zeng provided funding support, experimental design, data analysis, project supervision, and manuscript editing. All authors read and approved the final version of this manuscript.

Declaration of competing interest

The authors declare no conflicts of interest.

Acknowledgements

This research was funded by Natural Science Foundation of Guangdong Province (2018B030311012), Natural Science Foundation of China (82070811, 81770826), Sci-Tech Research Development Program of Guangzhou City (202201020497), National Key R&D Program of China (2017YFA0105803), and Key Area R&D Program of Guangdong Province (2019B020227003).

Appendix A. Supplementary data

Supplementary data to this article can be found online at https://doi.org/10.1016/j.livres.2023.05.003.

References

1. Pan XF, Wang L, Pan A. Epidemiology and determinants of obesity in China. *Lancet Diabetes Endocrinol*. 2021;9:373–392. https://doi.org/10.1016/S2213-8587(21)00045-0.
2. Loomba R, Sanyal AJ. The global NAFLD epidemic. *Nat Rev Gastroenterol Hepatol*. 2013;10:686–690. https://doi.org/10.1038/nrgastro.2013.171.
3. Younossi ZM, Koenig AB, Abdelatif D, Fazel Y, Henry L, Wymer M. Global epidemiology of nonalcoholic fatty liver disease-Meta-analytic assessment of prevalence, incidence, and outcomes. *Hepatology*. 2016;64:73–84. https://doi.org/10.1002/hep.28431.
4. Loomba R, Friedman SL, Shulman GI. Mechanisms and disease consequences of nonalcoholic fatty liver disease. *Cell*. 2021;184:2537–2564. https://doi.org/10.1016/j.cell.2021.04.015.
5. Anstee QM, Targher G, Day CP. Progression of NAFLD to diabetes mellitus, cardiovascular disease or cirrhosis. *Nat Rev Gastroenterol Hepatol*. 2013;10:330–344. https://doi.org/10.1038/nrgastro.2013.41.
6. Park SK, Seo MH, Shin HC, Ryoo JH. Clinical availability of nonalcoholic fatty liver disease as an early predictor of type 2 diabetes mellitus in Korean men: 5-year prospective cohort study. *Hepatology*. 2013;57:1378–1383. https://doi.org/10.1002/hep.26183.
7. Targher G, Corey KE, Byrne CD, Roden M. The complex link between NAFLD and type 2 diabetes mellitus - mechanisms and treatments. *Nat Rev Gastroenterol Hepatol*. 2021;18:599–612. https://doi.org/10.1038/s41575-021-00448-y.
8. Nasr P, Ignatova S, Kechagias S, Ekstedt M. Natural history of nonalcoholic fatty liver disease: a prospective follow-up study with serial biopsies. *Hepatol Commun*. 2017;2:199–210. https://doi.org/10.1002/hep4.1134.
9. Ferguson D, Finck BN. Emerging therapeutic approaches for the treatment of NAFLD and type 2 diabetes mellitus. *Nat Rev Endocrinol*. 2021;17:484–495. https://doi.org/10.1038/s41574-021-00507-z.
10. Adams LA, Lymp JF, St Sauver J, et al. The natural history of nonalcoholic fatty liver disease: a population-based cohort study. *Gastroenterology*. 2005;129:113–121. https://doi.org/10.1053/j.gastro.2005.04.014.
11. Younossi ZM, Golabi P, de Avila L, et al. The global epidemiology of NAFLD and NASH in patients with type 2 diabetes: a systematic review and meta-analysis. *J Hepatol*. 2019;71:793–801. https://doi.org/10.1016/j.jhep.2019.06.021.
12. Agius L. Targeting hepatic glucokinase in type 2 diabetes: weighing the benefits and risks. *Diabetes*. 2009;58:18–20. https://doi.org/10.2337/db08-1470.
13. Zhu D, Li X, Ma J, et al. Dorzagliatin in drug-naïve patients with type 2 diabetes: a randomized, double-blind, placebo-controlled phase 3 trial. *Nat Med*. 2022;28:965–973. https://doi.org/10.1038/s41591-022-01802-6.
14. Yang W, Zhu D, Gan S, et al. Dorzagliatin add-on therapy to metformin in patients with type 2 diabetes: a randomized, double-blind, placebo-controlled phase 3 trial. *Nat Med*. 2022;28:974–981. https://doi.org/10.1038/s41591-022-01803-5.
15. Zhu D, Gan S, Liu Y, et al. Dorzagliatin monotherapy in Chinese patients with type 2 diabetes: a dose-ranging, randomised, double-blind, placebo-controlled, phase 2 study. *Lancet Diabetes Endocrinol*. 2018;6:627–636. https://doi.org/10.1016/S2213-8587(18)30105-0.
16. Chorlton J, Hollowood Z, Dyer C, et al. A randomised, double-blind, placebo-controlled, multicentre clinical trial of AZD1656 in diabetic patients hospitalised with COVID-19: the ARCADIA Trial - implications for therapeutic immune modulation. *EClinicalMedicine*. 2022;51, 101604. https://doi.org/10.1016/j.eclinm.2022.101604.
17. Agius L. Glucokinase and molecular aspects of liver glycogen metabolism. *Biochem J*. 2008;414:1–18. https://doi.org/10.1042/BJ20080595.
18. Iynedjian PB. Molecular physiology of mammalian glucokinase. *Cell Mol Life Sci*. 2009;66:27–42. https://doi.org/10.1007/s00018-008-8322-9.
19. Malhi H, Kaufman RJ. Endoplasmic reticulum stress in liver disease. *J Hepatol*. 2011;54:795–809. https://doi.org/10.1016/j.jhep.2010.11.005.
20. Lebeaupin C, Vallée D, Hazari Y, Hetz C, Chevet E, Bailly-Maitre B. Endoplasmic reticulum stress signalling and the pathogenesis of non-alcoholic fatty liver disease. *J Hepatol*. 2018;69:927–947. https://doi.org/10.1016/j.jhep.2018.06.008.
21. Hetz C, Zhang K, Kaufman RJ. Mechanisms, regulation and functions of the unfolded protein response. *Nat Rev Mol Cell Biol*. 2020;21:421–438. https://doi.org/10.1038/s41580-020-0250-z.

22. Ajoolabady A, Kaplowitz N, Lebeaupin C, et al. Endoplasmic reticulum stress in liver diseases. *Hepatology*. 2023;77:619–639. https://doi.org/10.1002/hep.32562.
23. Liu X, Green RM. Endoplasmic reticulum stress and liver diseases. *Liver Res*. 2019;3:55–64. https://doi.org/10.1016/j.livres.2019.01.002.
24. Gregor MF, Yang L, Fabbrini E, et al. Endoplasmic reticulum stress is reduced in tissues of obese subjects after weight loss. *Diabetes*. 2009;58:693–700. https://doi.org/10.2337/db08-1220.
25. Puri P, Mirshahi F, Cheung O, et al. Activation and dysregulation of the unfolded protein response in nonalcoholic fatty liver disease. *Gastroenterology*. 2008;134:568–576. https://doi.org/10.1053/j.gastro.2007.10.039.
26. Rutkowski DT, Wu J, Back SH, et al. UPR pathways combine to prevent hepatic steatosis caused by ER stress-mediated suppression of transcriptional master regulators. *Dev Cell*. 2008;15:829–840. https://doi.org/10.1016/j.devcel.2008.10.015.
27. Xiao G, Zhang T, Yu S, et al. ATF4 protein deficiency protects against high fructose-induced hypertriglyceridemia in mice. *J Biol Chem*. 2013;288:25350–25361. https://doi.org/10.1074/jbc.M113.470526.
28. Eizirik DL, Cardozo AK, Cnop M. The role for endoplasmic reticulum stress in diabetes mellitus. *Endocr Rev*. 2008;29:42–61. https://doi.org/10.1210/er.2007-0015.
29. Shirakawa J, Togashi Y, Sakamoto E, et al. Glucokinase activation ameliorates ER stress-induced apoptosis in pancreatic β-cells. *Diabetes*. 2013;62:3448–3458. https://doi.org/10.2337/db13-0052.
30. Chen C, Matye D, Wang Y, Li T. Liver-specific microRNA-185 knockout promotes cholesterol dysregulation in mice. *Liver Res*. 2021;5:232–238. https://doi.org/10.1016/j.livres.2020.09.001.
31. Pettersson US, Waldén TB, Carlsson PO, Jansson L, Phillipson M. Female mice are protected against high-fat diet induced metabolic syndrome and increase the regulatory T cell population in adipose tissue. *PLoS One*. 2012;7, e46057. https://doi.org/10.1371/journal.pone.0046057.
32. Ford BE, Chachra SS, Alshawi A, et al. Chronic glucokinase activator treatment activates liver Carbohydrate response element binding protein and improves hepatocyte ATP homeostasis during substrate challenge. *Diabetes Obes Metab*. 2020;22:1985–1994. https://doi.org/10.1111/dom.14111.
33. Kennard MR, Nandi M, Chapple S, King AJ. The glucose tolerance test in mice: sex, drugs and protocol. *Diabetes Obes Metab*. 2022;24:2241–2252. https://doi.org/10.1111/dom.14811.
34. Kuate D, Kengne AP, Biapa CP, Azantsa BG, Abdul Manan Bin Wan Muda W. Tetrapleura tetraptera spice attenuates high-carbohydrate, high-fat diet-induced obese and type 2 diabetic rats with metabolic syndrome features. *Lipids Health Dis*. 2015;14:50. https://doi.org/10.1186/s12944-015-0051-0.
35. Zhu C, Huang M, Kim HG, et al. SIRT6 controls hepatic lipogenesis by suppressing LXR, ChREBP, and SREBP1. *Biochim Biophys Acta Mol Basis Dis*. 2021;1867, 166249. https://doi.org/10.1016/j.bbadis.2021.166249.
36. Matsuo M. ABCA1 and ABCG1 as potential therapeutic targets for the prevention of atherosclerosis. *J Pharmacol Sci*. 2022;148:197–203. https://doi.org/10.1016/j.jphs.2021.11.005.
37. Anderson CM, Stahl A. SLC27 fatty acid transport proteins. *Mol Aspects Med*. 2013;34:516–528. https://doi.org/10.1016/j.mam.2012.07.010.
38. Zheng X, Xu F, Liang H, et al. SIRT1/HSF1/HSP pathway is essential for exenatide-alleviated, lipid-induced hepatic endoplasmic reticulum stress. *Hepatology*. 2017;66:809–824. https://doi.org/10.1002/hep.29238.
39. Deniaud A, Sharaf el dein O, Maillier E, et al. Endoplasmic reticulum stress induces calcium-dependent permeability transition, mitochondrial outer membrane permeabilization and apoptosis. *Oncogene*. 2008;27:285–299. https://doi.org/10.1038/sj.onc.1210638.
40. Malhi H, Kropp EM, Clavo VF, et al. C/EBP homologous protein-induced macrophage apoptosis protects mice from steatohepatitis. *J Biol Chem*. 2013;288:18624–18642. https://doi.org/10.1074/jbc.M112.442954.
41. Deshpande AM, Bhuniya D, De S, et al. Discovery of liver-directed glucokinase activator having anti-hyperglycemic effect without hypoglycemia. *Eur J Med Chem*. 2017;133:268–286. https://doi.org/10.1016/j.ejmech.2017.03.042.
42. Katz L, Manamley N, Snyder WJ, et al. AMG 151 (ARRY-403), a novel glucokinase activator, decreases fasting and postprandial glycaemia in patients with type 2 diabetes. *Diabetes Obes Metab*. 2016;18:191–195. https://doi.org/10.1111/dom.12586.
43. Meininger GE, Scott R, Alba M, et al. Effects of MK-0941, a novel glucokinase activator, on glycemic control in insulin-treated patients with type 2 diabetes. *Diabetes Care*. 2011;34:2560–2566. https://doi.org/10.2337/dc11-1200.
44. Kawata S, Nakamura A, Miyoshi H, et al. Glucokinase activation leads to an unsustained hypoglycaemic effect with hepatic triglyceride accumulation in db/db mice. *Diabetes Obes Metab*. 2022;24:391–401. https://doi.org/10.1111/dom.14586.
45. Lin YC, Chang PF, Chang MH, Ni YH. Genetic variants in GCKR and PNPLA3 confer susceptibility to nonalcoholic fatty liver disease in obese individuals. *Am J Clin Nutr*. 2014;99:869–874. https://doi.org/10.3945/ajcn.113.079749.
46. Santoro N, Zhang CK, Zhao H, et al. Variant in the glucokinase regulatory protein (GCKR) gene is associated with fatty liver in obese children and adolescents. *Hepatology*. 2012;55:781–789. https://doi.org/10.1002/hep.24806.
47. Anstee QM, Seth D, Day CP. Genetic factors that affect risk of alcoholic and nonalcoholic fatty liver disease. *Gastroenterology*. 2016;150:1728–1744(e7). https://doi.org/10.1053/j.gastro.2016.01.037.